

This item is the archived peer-reviewed author-version of:

Three-dimensional movement of the beak during seed processing in domestic canaries

Reference:

Mielke Maja, Van Wassenbergh Sam.- Three-dimensional movement of the beak during seed processing in domestic canaries
The journal of experimental biology - ISSN 1477-9145 - 225:14(2022), jeb244360
Full text (Publisher's DOI): <https://doi.org/10.1242/JEB.244360>
To cite this reference: <https://hdl.handle.net/10067/1893090151162165141>

THREE-DIMENSIONAL MOVEMENT OF THE BEAK DURING SEED PROCESSING IN DOMESTIC CANARIES**Running title:** Beak movement in feeding canaries**Authors:**Maja Mielke¹, corresponding author (maja.mielke.bio@mailbox.org), ORCID: 0000-0001-6328-0589Sam Van Wassenbergh¹, ORCID: 0000-0001-5746-4621¹ Laboratory of Functional Morphology, Department of Biology, Faculty of Sciences, University of Antwerp, 2610 Wilrijk, Belgium**Key words:** Beak movement, feeding, kinematics, seed cracking, songbirds**Summary statement**

Domestic canaries apply specific three-dimensional movements of their upper and lower beaks during the various phases of seed processing. This includes extremely fast open-close frequencies during phases of seed positioning.

1
2
3
4
5
6
7
8
9
10
11
12
13
14

1 RESEARCH ARTICLE

2 Three-dimensional movement of the beak during seed
3 processing in domestic canaries4 Maja Mielke¹ and Sam Van Wassenbergh¹
56 ABSTRACT
7

8 Many songbird species rely on seeds as a primary food source and the process of picking up, positioning, cracking, dehusking, and
9 swallowing seeds is one of the most sophisticated tasks of the beak. Still, we lack understanding about how granivorous songbirds
10 move their beak during the different phases of seed processing. In this study, we used multi-view high speed imaging to analyze
11 the three-dimensional movement of the beak in feeding domestic canaries. Our analysis focuses on correlation of upper and lower
12 beak, frequency of mandibulation, and direction of mandible movement in 3D space. We show that the correlation of maxilla and
13 mandible movement differs among the phases of seed processing. Furthermore, we found that the beak moves at extremely high
14 frequencies, up to 25 Hz, which resembles previously reported maximal syllable rates in singing canaries. Finally, we report that
15 canaries use specific 3D mandible movements during the different phases of seed processing. Kinematic parameters do not differ
16 between male and female canaries. Our findings provide an important biomechanical basis for better understanding the beak as a
17 functional tool.

18 **KEYWORDS:** beak movement, feeding, kinematics, seed cracking, songbirds
19

20 INTRODUCTION

21 In granivorous songbirds, efficient cracking and dehusking of seeds is essential for meeting the high energy demands and minimizing
22 exposure to predators by reducing foraging times. The ability of birds to successfully crack certain types of seeds is largely determined
23 by beak size and shape, as has been mostly described in Darwin's finches (Grant, 1981; Grant and Grant, 1995; Herrel et al., 2005),
24 but also in other songbirds (Kear, 1962; Ziswiler, 1965; Smith, 1987). In seed cracking birds, not only the outer shape, but also the
25 inner beak morphology is adapted to a granivorous diet, showing specialized grooves and edges on the horny palate aiding in seed
26 immobilisation (Ziswiler, 1965) and adapted trabecular bone within the bony part of the beak improving mechanical resistance during
27 biting (Genbrugge et al., 2012). For very hard seeds, birds need a sufficient bite force, which is related to beak morphology (Herrel et al.,
28 2005), skull morphology (van der Meij and Bout, 2008), and jaw muscle size (van der Meij and Bout, 2004; Genbrugge et al., 2011).
29 Furthermore, feeding on hard seeds requires beak and skull to withstand demanding loading regimes to avoid fractures (Soons et al.,
30 2010; 2015).

31 Different songbirds show different efficiency and techniques in cracking the same type of seeds (Kear, 1962; Grant, 1981; van der Meij
32 and Bout, 2006). Small-billed birds need longer for processing large and hard seeds. Large-billed birds, however, are also less efficient
33 and less successful in handling small seeds (Abbott et al., 1975; Smith, 1987), presumably because they have difficulties positioning
34 small seeds for cracking (Abbott et al., 1975). To meet their high energy demands, small-billed birds need to compensate their inability
35 to crack large seeds that exceed their bite force by a high frequency of consumption of small seeds. (Benkman and Pulliam, 1988).
36 Furthermore, they use seed size characteristics to predict seed hardness and selectively choose seeds that are in the range of their biting
37 abilities (van der Meij and Bout, 2000).

38 Adaptations to produce high bite forces and crack hard seeds impose constraints on beak movement in general. Kinematic analyses of
39 beak movement during singing have revealed that songbirds with a high bite force move their beak at lower frequencies and produce
40 songs of lower frequency bandwidths than birds with low bite force (Podos, 2001; Huber and Podos, 2006; Herrel et al., 2009). In

¹Laboratory of Functional Morphology, Department of Biology, Faculty of Sciences, University of Antwerp, 2610 Wilrijk, Belgium

contrast, small-billed songbirds with low bite forces, like domestic canaries (Fringillidae, 'true finches'), move their beak extremely fast (up to 30 Hz) during singing (Drăgănoiu et al., 2002). Such high beak agility should be beneficial for a successful feeding on small seeds in canaries. In order to test this, kinematic analyses of beak movement during feeding is needed, which will help to reveal whether feeding and singing behavior share similar performance constraints.

In contrast to mammals, both the upper jaw (maxilla) and the lower jaw (mandible) contribute to gape opening in birds. The elevation of the maxilla is called cranial kinesis, which can occur via a rotation around the naso-frontal hinge (prokinesis) or via bending zones along the dorsal bar of the maxilla (rhynchokinesis, Bock, 1964). Maxilla elevation is induced via a forward rotation of the quadrate bones, which protract the jugal bones and the pterygoid–palatinum complex, and is thus only possible because the avian cranium is highly kinetic. In some species, a coupling mechanism has been described that induces maxilla elevation when the mandible is depressed, resulting in a synchronized movement of mandible and maxilla (Bock, 1964; Zusi, 1967). However, the exact mechanism of coupling is still not fully resolved. Bock (1964) has suggested that inextensible ligaments like the postorbital ligament (PO ligament) or functionally equivalent ligaments induce coupled kinesis via restriction of mandible depression. Zusi (1967), however, has shown in domestic chicken and evening grosbeaks that the coupled coordination of upper and lower beak does not require a PO ligament and can even be induced by activation of the *M. depressor mandibulae* alone. In zebra finches, the PO ligament has been shown to contribute only 20% of total resistance force (Nuijens and Bout, 1998), which makes a central role of this ligament in coupled kinesis unlikely in that species. Furthermore, in white-throated sparrows, maxilla and mandible movement can be completely independent (uncoupled kinesis), although a PO ligament is present (Hoese and Westneat, 1996). Many studies on beak kinematics during singing or feeding do not allow for an analysis of coupled kinesis, because only gape distance and/or gape angle are recorded (e.g., Westneat et al., 1993; Bout and Zeigler, 1994; van der Meij and Bout, 2008; Neves et al., 2019). To analyze whether maxilla and mandible movement are coupled or not, movement of upper and lower beak needs to be recorded separately relative to a common reference frame (cf. van der Meij and Bout, 2006). Suchlike analysis, combined with anatomical knowledge of the species, is needed to identify how specific cranial morphologies relate to coupling of beak movement.

During seed processing, the beak can move in a way that goes far beyond a mere open-close mechanism. In particular, for an efficient positioning, cracking, and dehusking of seeds, the lower beak can perform medio-lateral movement, as has been described in different fringillids (Ziswiler, 1965; Nuijens and Zweers, 1997; van der Meij and Bout, 2006), but the extent to which medio-lateral movement is used depends on the species and cracking techniques. It has been suggested that the absence of a PO ligament can facilitate medio-lateral movement of the mandible during seed dehusking (Nuijens and Zweers, 1997; Nuijens and Bout, 1998). This would be in line with the findings of comparative studies on two families of granivorous passerine birds, Fringillidae and Estrildidae. These studies showed that medio-lateral movement occurs in fringillid species, which don't have a (fully developed) PO ligament, but none in estrildid species, which have a PO ligament (e.g., Nuijens and Zweers, 1997; van der Meij and Bout, 2006). Most studies on beak kinematics, e.g. of singing, are only based on lateral recordings, allowing for an analysis of movement in the sagittal plane only (but see e.g., Gussekkloo et al., 2001, for an *ex vivo* study of 3D kinematics). Consequently, *in vivo* medio-lateral movement of the mandible has only been described qualitatively so far, if at all (but see van der Meij and Bout, 2006, for a preliminary analysis). Three-dimensional video recordings of beak movement are necessary to assess beak movement in all planes. Analyzing how songbirds utilize the full range of motion of their beak during tasks like seed cracking will contribute to our knowledge on the functional adaptation of the beak and the underlying cranial system.

In this study, we use multi-view high speed videography of feeding domestic canaries to test the following hypotheses about the three-dimensional movement of the beak in a granivorous songbird. Firstly, we hypothesize that upper and lower jaw movement are coupled, because this has been reported for another fringillid songbird before (Zusi, 1967). Secondly, we hypothesize that maximal beak movement frequencies during feeding are similar to those during the fastest song fragments. This is expected because of the sexual selection favoring fast songs in domestic canaries (Drăgănoiu et al., 2002). Thirdly, we hypothesize that domestic canaries utilize medio-lateral movement of the mandible during seed processing. This is especially expected for cracking attempts (cf. van der Meij and Bout, 2006) and during seed husk removal (cf. Ziswiler, 1965).

Our results provide novel insights into the beak kinematics of a granivorous songbird and help to understand how they are functionally adapted to a mechanically demanding and sophisticated task like seed cracking.

86 MATERIALS AND METHODS

87 Study species

88 In this study, six individuals (three females, three males) of domestic canaries (*Serinus canaria domestica*, Fife Fancy breed) were used.
89 Birds of the genus *Serinus* are small granivorous passerine birds that belong to the finch family Fringillidae. The domestic canaries
90 used for this study were from a lab-bred population of the Behavioral Ecology and Ecophysiology Research group at the University of
91 Antwerp, Belgium. The birds were born in 2016 and experiments were performed between March and October 2021. Birds were housed
92 individually in cages (60x50x40 cm) with water and standard seed mix available *ad libitum*. All experiments described in this study were
93 approved by the Ethical Committee for Animal Testing of the University of Antwerp (ECD code: 2020-40).

94

95 Recording setup and experimental procedure

96 Video recordings were made at 500 frames per second using four synchronized high speed cameras (FASTEC-IL5, Fastec Imaging from
97 San Diego, USA) with 35 mm f1.7 lenses and a shutter speed of 100 μ s. The four cameras were filming the birds from four different
98 angles in 2x2 arrangement. The feeder was positioned in a way that the birds were, while looking ahead, facing the center of the 2x2
99 camera setup (Fig. 1A). Illumination was provided by near-infrared LED spots. Videos were stored as series of tiff images (936x1024
100 pixels). During recording, birds were in a glass cage containing bird sand, a long perch, water, and a feeder with a short perch for sitting
101 on while feeding. The feeder was positioned in a way that when the birds came sitting on the short perch, their beak was likely positioned
102 in the center of the small focus volume. Before and after each recording session, 20-30 calibration images of a self-made 3D-calibration
103 fixture were recorded. This allowed us to later reconstruct the beak movement in 3D space.

104 19 h prior to the recording session, birds were transferred to the glass recording cage where they were deprived of food, but had access
105 to water *ad libitum*. Before starting the recording, markers were applied with a fine black ink pen on maxilla, mandible, and head of the
106 birds. Seven and five markers were applied on maxilla and mandible, respectively, and six markers on the head (drawn on a piece of
107 adhesive tape that was attached on the crown of the birds, see Figs 1B,C). The canaries were offered hemp seeds (*Cannabis sativa*) in a
108 small Petri dish (35x10 mm) on the feeder. Whenever the bird hopped on the short feeder perch and started feeding, video recording was
109 started manually via an external trigger and paused whenever the bird left the feeder. In addition to feeding, short sequences of the birds
110 with a closed beak were recorded to determine the reference position of maxilla-, mandible-, and head markers relative to each other.
111 The session was stopped when the bird stopped feeding or after a maximum duration of one hour, after which animals were returned to
112 their home cage.

113 Video selection and digitization

114 From the raw video material, only successful feeding attempts were extracted (where the seed was cracked, dehusked, and swallowed).
115 The start of a feeding sequence was defined as the moment when the beak starts to open for picking up the seed and the end was defined as
116 the moment when the seed is fully swallowed (cf. supplementary movie S1). Because the head markers were used to define the reference
117 frame of maxilla- and mandible movement, videos were discarded when head markers were not fully visible. Camera calibration and
118 marker tracking were done in XMALab (Knörlein et al., 2016). For marker tracking, dot detection was used, which successfully detected
119 the markers on a great majority of frames. Where necessary, tracking was corrected manually, using reprojection errors and marker-
120 to-marker distances as indicators for incorrectly tracked markers. The final mean reprojection error was 0.34 pixels. Each marker was
121 tracked in at least two camera views to allow calculation of 3D coordinates. Additionally, the different phases of each feeding event were
122 marked in XMALab. We distinguished the four phase types 'positioning', 'biting', 'dehusking', and 'swallowing' (supplementary movie
123 S1). During positioning, the seed lies rather loose in the beak and is rotated by the tongue to bring it into the right position for a cracking
124 attempt. During biting (the actual cracking attempt), the seed is fixed in an upright position between maxilla and mandible, with the
125 natural seed margins aligned with the edges of upper and lower beak. In a successful trial, positioning and biting phases are alternately
126 repeated until the shell is cracked open. Note that each repetition of positioning or biting within one feeding event accounts for a single
127 data point later on. During the dehusking phase, the two major halves of the shell are removed from the seed. The swallowing phase
128 involves removal of small remains of the shell and swallowing of the seed. The feeding phases, together with the 3D marker coordinates,
129 were exported from XMALab for further processing. In total, 16 feeding events from six individuals (3 males, 3 females) were analyzed.
130 The data include 79 positioning phases, 80 biting phases, 16 dehusking phases, and 15 swallowing phases.

Preprocessing of 3D marker coordinates

131

The 3D marker coordinates of closed beak and feeding events were imported into Python (Python Software Foundation, 2022) where all the subsequent analyses were performed. First, in order to be able to assess beak movement along the anatomical axes of the head, the 3D marker coordinates needed to be adjusted accordingly. We used the point cloud of the 18 reference markers from the closed beak recordings to define the coordinate system. To do so, we rotated this closed beak marker point cloud in a way that the six head markers are in the XY-plane; the YZ-plane was defined by the dorsal and ventral markers of maxilla and mandible, respectively (Fig. 1B). In order to bring the 3D data of the feeding events into this coordinate system, we aligned the six head markers of each frame with the head markers of the aligned closed beak reference via Procrustes superimposition (Rohlf and Slice, 1990). By doing so, the head movement of the birds was removed from the data and all the remaining signal was only the beak movement. Furthermore, this alignment allowed us to analyze maxilla- and mandible movement separately by calculating the displacement of maxilla- and mandible markers from their reference positions on the closed beak (see Fig. 1D). Due to the definition of the reference coordinate system, displacement in X-, Y-, and Z-direction then corresponds to medio-lateral, antero-posterior, and dorso-ventral displacement, respectively. By plotting ΔZ (Fig. 1E) of maxilla and mandible over time, one can visualize qualitative gape change during the different phases of the feeding event. Displacement data (ΔX , ΔY , and ΔZ) were low-pass-filtered using a Butterworth filter (threshold 60 Hz). For each frame of a phase (as shown in the upper row of Fig. 1E), we averaged the displacement of only those markers that were visible during the whole duration of that phase to omit artifacts due to appearing or disappearing of individual markers. The filtered and Procrustes-aligned beak movement data (ΔX , ΔY , and ΔZ of maxilla and mandible of all feeding events) are available in Dryad. Note that, because the absolute values of these averaged ΔZ partly depend on the number and positions of visible markers during that phase, this analysis does not allow for a calculation of actual gape distance, but instead provides information about the qualitative beak movement over time. Due to the averaging of the displacement of several markers, we remain with only one ΔX , ΔY , and ΔZ value per rigid body (maxilla or mandible) per frame interval. These averaged displacement values were used for the calculation of further beak movement parameters (see below).

Calculation of beak movement parameters

152

We focused on three main questions when analyzing the displacement data (ΔX , ΔY , and ΔZ). (1) How strongly are maxilla and mandible movement correlated during the different phases of seed processing? (2) How fast does the beak move, i.e., how many oscillations occur per second? (3) How much percent of displacement per frame interval occurs in medio-lateral, antero-posterior, and dorso-ventral direction and do percentages differ among the phases of seed processing?

To assess correlation, we calculated the correlation coefficient of maxilla- and mandible displacement in dorso-ventral direction (ΔZ) for the individual feeding phases. Negative correlation coefficients indicate opposite movement (e.g., maxilla elevation coincides with mandible depression), positive values indicate paralleled movement (e.g., maxilla elevation coincides with mandible elevation). The higher the absolute value, the higher the synchronization in both cases.

To assess the number of beak oscillations per second, we calculated the frequency of mandible movement in dorso-ventral direction (ΔZ) using the Welch method (*signal.welch()* function of the SciPy library, Virtanen et al., 2020) in Python. This was only done for the positioning phases, because here the beak moves fastest, with the highest amplitude, and most regularly compared to the other phases.

To assess the relative displacement of the mandible in X-, Y-, and Z-direction (i.e., to quantify 3D movement direction), we calculated for each frame f the percentage M of X-, Y-, and Z-displacement relative to frame $f - 1$. M was calculated as follows:

$$M \begin{pmatrix} \Delta X_f \\ \Delta Y_f \\ \Delta Z_f \end{pmatrix} = \frac{\delta \cdot 100\%}{\sum_i \delta_i} \quad (1)$$

with

$$\delta = \begin{pmatrix} \Delta X_f - \Delta X_{f-1} \\ \Delta Y_f - \Delta Y_{f-1} \\ \Delta Z_f - \Delta Z_{f-1} \end{pmatrix} \quad (2)$$

169 Note that $M(\Delta X_f)$, $M(\Delta Y_f)$, and $M(\Delta Z_f)$ always add up to 100% and are independent of gape angle, because M considers
170 displacement relative to each previous frame rather than relative to the closed beak reference position. Values of $M(\Delta X_f)$, $M(\Delta Y_f)$, and
171 $M(\Delta Z_f)$ were averaged for each individual phase of a feeding event. All calculated beak movement parameters (correlation coefficients,
172 frequency, and percental mandible displacement) are available in Dryad.

173 Statistical analyses

174 Statistical analysis was conducted in Python using the probabilistic programming package PyMC (version 4.0.0, Salvatier et al., 2016).
175 For the correlation coefficient c , mandible frequency f , and percental mandible displacement m , we tested different models and per-
176 formed model comparison with Leave-One-Out cross-validation (PSIS-Loo, cf. Vehtari et al., 2017) to assess which model best fits to
177 the data (see Table 1). The Python code of the modeling is available in Dryad.

178 Since correlation coefficients c are restricted to the interval $[-1,1]$, we selected a continuous distribution function with lower and upper
179 limits for the modeling process. Given a transformation of the correlation coefficients to the interval $[0,1]$ ($c_{trafo} = (c + 1)/2$), the
180 logit-normal distribution serves this purpose. We compared five different models (Table 1). Model C_{pool} fitted the logit-normal function
181 to the pooled data of all correlation coefficients. Model C_{sex} included 'sex' as a categorical variable, model C_{ph} included 'phase' as a
182 categorical variable, model $C_{sex,ph}$ included both 'sex' and 'phase' as categorical variables. Model $C_{sex/ph}$ was an interaction model,
183 considering all combinations of 'sex' and 'phase' as categorical variables.

184 For analyzing the frequency of dorso-ventral mandible movement, we fitted a Rice distribution, which is a continuous distribution func-
185 tion limited to positive values. The Rice distribution scored slightly better in model comparison than a Gamma function, which would be
186 limited to positive values as well. Because frequency was calculated solely for the positioning phases, only the models F_{pool} and F_{sex}
187 were evaluated (Table 1).

188 Percental mandible displacement is another parameter limited to a fixed interval $[0,100]$. Thus, a logit-normal distribution was used as
189 for the correlation coefficients, after transforming the percentages to the interval $[0,1]$ via $m_{trafo} = m/100$. Following the approach
190 used for correlation c , we compared the models M_{pool} , M_{sex} , M_{ph} , $M_{sex,ph}$, and $M_{sex/ph}$ (Table 1).

191 Note that, as we recorded only three individuals per sex, our data were not sufficient to statistically quantify the effect of individual
192 variation on beak kinematics. For test purposes, we analyzed the effect of including 'individual' as variable instead of 'sex'. During
193 model comparison, 'individual' models scored worse than or equally well as 'sex' models. This indicates that the former set of models
194 is less suited to reliably describe the effects seen in the data, which might be due to a true lack of individual variance, but more likely
195 points at limitations with regard to possible model complexity for the given sample size. Thus, the variable 'individual' was not included
196 in the models.

197 Dissection

198 Two canaries that had died naturally were used for a dissection of the head. The birds were from the same lab-bred population as our study
199 subjects and of the same age. According to the literature (Nuijens and Zweers, 1997), the PO ligament is absent or weakly developed in
200 Fringillidae. However, we had not found evidence about that for domestic canaries in particular. Hence, the goal of the dissection was to
201 confirm that the canaries don't have a PO ligament. Furthermore, we used the cadavers to test the cranium for a coupling mechanism via
202 manipulation of the beak.

203 RESULTS

204 Correlation of maxilla and mandible movement depends on the phase of seed processing

205 In order to assess to what extent the dorso-ventral movement of maxilla and mandible are correlated, we calculated the correlation
206 coefficient c of their ΔZ trajectories (cf. Fig. 1E) for the different phases ('positioning', 'biting', 'dehusking', and 'swallowing'). During
207 positioning and swallowing, c was mostly negative (-0.66 ± 0.16 and -0.25 ± 0.21 , respectively; Fig. 2). During dehusking and biting, c was
208 more variable, covering both negative and positive values (-0.21 ± 0.34 and -0.11 ± 0.32). Correlation was affected by the phase, but not
209 by sex; models C_{pool} and C_{sex} scored equally in model comparison, but C_{ph} much better than both (Table 1). Adding 'sex' as a second
210 categorical variable, either independently ($C_{sex,ph}$) or in combination with 'phase' ($C_{sex/ph}$), did not improve the outcome considerably
211 (Table 1). We conclude that in domestic canaries, there is no obligate coupling of beak movement and the amount of correlation depends
212 on the phase of seed processing, but not on the sex.

Table 1. Definitions of statistical models used for the different parameters and results of model comparison.

Model	Model description	rank	LOO \pm se	d_LOO \pm se
$C_{sex/ph}$	$c \sim \sum_{sex} \sum_{ph} \nu_{sex,ph} \beta_{sex,ph} + \epsilon$	0	140 \pm 10	0 \pm 0
$C_{sex,ph}$	$c \sim \alpha + \nu_{male} \beta_{male} + \sum_{ph \neq pos} \nu_{ph} \beta_{ph} + \epsilon$	1	136 \pm 9	4 \pm 2
C_{ph}	$c \sim \alpha + \sum_{ph \neq pos} \nu_{ph} \beta_{ph} + \epsilon$	2	135 \pm 9	5 \pm 3
C_{sex}	$c \sim \alpha + \nu_{male} \beta_{male} + \epsilon$	3	72 \pm 7	68 \pm 7
C_{pooled}	$c \sim \alpha + \epsilon$	4	72 \pm 7	69 \pm 7
F_{pool}	$f \sim \alpha + \epsilon$	0	-215 \pm 5	0 \pm 0
F_{sex}	$f \sim \alpha + \nu_{male} \beta_{male} + \epsilon$	1	-216 \pm 5	1 \pm 1
$M_{sex/ph}(X)$	$m_x \sim \sum_{sex} \sum_{ph} \nu_{sex,ph} \beta_{sex,ph} + \epsilon$	0	350 \pm 9	0 \pm 0
$M_{ph}(X)$	$m_x \sim \alpha + \sum_{ph \neq pos} \nu_{ph} \beta_{ph} + \epsilon$	1	334 \pm 10	16 \pm 5
$M_{sex,ph}(X)$	$m_x \sim \alpha + \nu_{male} \beta_{male} + \sum_{ph \neq pos} \nu_{ph} \beta_{ph} + \epsilon$	2	334 \pm 11	16 \pm 6
$M_{pool}(X)$	$m_x \sim \alpha + \epsilon$	3	271 \pm 8	79 \pm 7
$M_{sex}(X)$	$m_x \sim \alpha + \nu_{male} \beta_{male} + \epsilon$	4	270 \pm 8	80 \pm 7
$M_{sex/ph}(Y)$	$m_y \sim \sum_{sex} \sum_{ph} \nu_{sex,ph} \beta_{sex,ph} + \epsilon$	0	335 \pm 10	0 \pm 0
$M_{ph}(Y)$	$m_y \sim \alpha + \sum_{ph \neq pos} \nu_{ph} \beta_{ph} + \epsilon$	1	321 \pm 10	14 \pm 5
$M_{sex,ph}(Y)$	$m_y \sim \alpha + \nu_{male} \beta_{male} + \sum_{ph \neq pos} \nu_{ph} \beta_{ph} + \epsilon$	2	320 \pm 9	15 \pm 5
$M_{pool}(Y)$	$m_y \sim \alpha + \epsilon$	3	232 \pm 7	103 \pm 10
$M_{sex}(Y)$	$m_y \sim \alpha + \nu_{male} \beta_{male} + \epsilon$	4	231 \pm 7	105 \pm 10
$M_{sex/ph}(Z)$	$m_z \sim \sum_{sex} \sum_{ph} \nu_{sex,ph} \beta_{sex,ph} + \epsilon$	0	280 \pm 8	0 \pm 0
$M_{ph}(Z)$	$m_z \sim \alpha + \sum_{ph \neq pos} \nu_{ph} \beta_{ph} + \epsilon$	1	268 \pm 9	12 \pm 5
$M_{sex,ph}(Z)$	$m_z \sim \alpha + \nu_{male} \beta_{male} + \sum_{ph \neq pos} \nu_{ph} \beta_{ph} + \epsilon$	2	267 \pm 8	12 \pm 4
$M_{pool}(Z)$	$m_z \sim \alpha + \epsilon$	3	149 \pm 6	131 \pm 9
$M_{sex}(Z)$	$m_z \sim \alpha + \nu_{male} \beta_{male} + \epsilon$	4	148 \pm 6	132 \pm 9

The column 'Model description' describes the models as they were implemented in the statistical analysis. The 'rank' column shows the rank of the models after model comparison, starting from 0 (best model). The 'LOO' column shows the values of the Leave-One-Out cross-validation (LOO \pm s.e.). The higher the LOO, the better the model. The 'd_LOO' column shows the difference (\pm s.e.) of each model to the best ranking model. Values are rounded. Note that models accounting for phase type ('ph', 'sex,ph', 'sex/ph') always score best and that differences among these 'ph' model variants are low.

Coupled kinesis is possible without a postorbital ligament

213

In order to confirm the absence of a PO ligament in canaries and to test for a coupling mechanism via manipulation of the beak, two canaries were dissected. We did not find a PO ligament in the birds. Unrestricted depression of the mandible by pulling the tip of the mandible down did not induce maxilla elevation. However, an upward push at the proximal side of the mandible while pulling it down at the mandible tip induced coupled kinesis of lower and upper beak. We conclude that, although a PO ligament is missing, coupled kinesis can occur as a result of forces in the dorsal direction applied to the mandible during beak opening.

The mandible moves with a frequency of up to 25 Hz during the positioning phase

219

In order to assess the number of mandible oscillations per second during the positioning phases, we calculated the frequency of dorso-ventral mandible movement ΔZ . The mandible moved with a frequency of 18 ± 4 Hz during positioning, ranging from 10 Hz up to 25 Hz. Statistical analysis revealed that the model F_{sex} did not score better than model F_{pool} , indicating that the sex did not affect frequency of mandible movement (Table 1). The observed frequencies lie within the range of reported syllable rates of singing domestic canaries (Drăgănoiu et al., 2002, , Fig. 3). We conclude that domestic canaries move their beak extremely fast during seed positioning, but the frequency does not differ between males and females.

Canaries use specific 3D mandible movements during different phases of seed processing

226

In order to determine how much the mandible moves in each of the three dimensions, we calculated the percentage of medio-lateral, antero-posterior, and dorso-ventral mandible movement for the different phases ('positioning', 'biting', 'dehusking', and 'swallowing') of each feeding event. The canaries used mostly dorso-ventral movement, but to different extent depending on the phase type. Dorso-ventral direction of mandible movement was more dominant during positioning ($64 \pm 5\%$) and swallowing ($59 \pm 5\%$) than during dehusking ($49 \pm 7\%$) and biting ($44 \pm 7\%$; Fig. 4). This is mainly because during dehusking and biting, more mandible movement was performed in medio-lateral direction. The percental values of all three dimensions were mainly affected by the phase: the three models which include phase as categorical variables ($M_{sex/ph}$, M_{ph} , and $M_{sex,ph}$) scored best in model comparison (Table 1). The differences in score among these three models were low compared to the differences to the models M_{pool} and M_{sex} , indicating that including 'sex' as a categorical

235 variable added little benefit to the model score. We conclude that domestic canaries, independent of sex, use specific three-dimensional
236 mandible movements for the different phases of seed processing.

237 DISCUSSION

238 Summary

239 The goal of this study was to test functional hypotheses about the beak movement during seed processing in a granivorous songbird. We
240 used multi-view high speed videography to reconstruct the three-dimensional movement of upper and lower beak in domestic canaries.
241 Our analysis focused on the correlation of upper and lower beak, frequency of beak movement, and the three-dimensional directions of
242 mandible movement during seed processing. We have shown that there is no obligate correlation of maxilla- and mandible movement.
243 Still, coupled kinesis is possible, given that mandible depression is restricted. The mandible moves at extremely high frequencies, with
244 up to 25 Hz, and specific 3D movements are used for the different phases of seed processing.

245 Mechanisms of cranial kinesis

246 We have shown that during feeding, maxilla and mandible movement is not always correlated in domestic canaries. While we observed a
247 mostly negative correlation of dorso-ventral movement during the positioning and swallowing phase, maxilla and mandible moved partly
248 independently during biting and dehusking. Cadaver manipulation revealed that there is probably no obligate coupling mechanism, but
249 coupled kinesis could be induced by restricting mandible depression.

250 We had hypothesized that beak movement is coupled in domestic canaries. This was based on the findings by Zusi (1967) that coupled
251 cranial kinesis is independent of the presence of a PO ligament and that activation of the *M. depressor mandibulae* suffices to induce
252 cranial kinesis in anesthetized fringillid finches. This was only partly confirmed in our study; the degree of coupling varied among phase
253 types and during cadaver manipulation, unrestricted mandible depression alone did not induce cranial kinesis. Our finding that correlation
254 of upper and lower jaw movement is not obligate during feeding suggests that domestic canaries can actively vary beak correlation
255 by adjusting beak movement according to the specific needs of each phase of seed processing.

256 Interestingly, not only the average correlation coefficient differed among phase types, but also the variation of correlation (Fig. 2), being
257 higher during biting and dehusking. During these phases, the beak has firm contact with the seed, which is necessary for opening and
258 removing the shell. The higher variation of correlation during these phases indicates the ability of the bird to flexibly control beak move-
259 ment according to the specific size, hardness, and position of each individual seed. Note that this higher variation in correlation coincides
260 with a higher amount of medio-lateral mandible movement during biting and dehusking (Fig. 4). During positioning and swallowing,
261 however, the seed lies rather loose in the beak and is manipulated more with the tongue than with the beak itself. Thus, the beak move-
262 ments are more standardized and correlation is less variable.

263 The possibility of coupled cranial kinesis in the domestic canary, a fringillid finch, challenges the hypothesis by Bock (1964) that cou-
264 pled beak movement depends on an inextensible PO ligament. Previous studies have partly questioned this key role of the PO ligament
265 in coupled kinesis as well. For example, the resistance force of the PO ligament has been shown to be too low to be able to actually
266 block mandible depression (Bout and Zweers, 2001; Nuijens and Bout, 1998). Furthermore, birds with a PO ligament do not necessarily
267 show coupled kinesis: maxilla and mandible can move independently in white-throated sparrows, although they have a PO ligament
268 (Hoese and Westneat, 1996). Also in chicken (*Gallus gallus domesticus*), coupled cranial kinesis does not dominate beak movement
269 during feeding, despite a PO ligament being present. This is because the maxilla is elevated actively via quadrate protractor muscles
270 which become active even before mandible depressor muscles, leaving the PO ligament unloaded (Van Den Heuvel, 1991). Similarly, in
271 mallard ducks (Dawson et al., 2011) and pigeons (Bout and Zeigler, 1994), maxilla elevation precedes mandible depression, deviating
272 from the mechanism suggested by Bock (1964). In conclusion, the presence of a PO ligament does not necessarily imply coupled cranial
273 kinesis.

274 We have shown that beak movement in domestic canaries can be correlated, especially during seed positioning and swallowing, and that
275 coupled cranial kinesis occurs if mandible depression is restricted. We propose two possible underlying mechanisms that are independ-
276 ent of a PO ligament. Either the maxilla is elevated independently via quadrate and pterygoid protractor muscles in a synchronized
277 way together with mandible depressors (cf. Hoese and Westneat, 1996), or coupled cranial kinesis is induced via a sufficiently anteriorly
278 directed line of action of the mandible depressor muscles to cause simultaneous quadrate protraction, potentially assisted by resisting
279 forces from the jaw adductors (cf. Bout and Zeigler, 1994; Van Gennip and Berkhoudt, 1992; Zusi, 1967). As the strongest coupling
280 is observed during the phase in which the highest accelerations of mandible depression is observed, namely the seed positioning phase

(Fig. 1E; Fig. 2), such a dynamic effect induced by depressor mandibulae forces seems possible. 281
 In general, however, the complexity of this mechanism demands caution in interpreting kinematic observations. It is likely that a cou- 282
 pling mechanism depends on a variety of factors such as species, gape angle, presence and mechanical properties of ligaments and cranial 283
 muscles, morphology and arrangement of cranial bones, etc. This prohibits generic conclusions about this mechanism in songbirds and 284
 even fringillids in general. Further research is needed to reliably identify the actual underlying mechanism of coupled cranial kinesis in 285
 domestic canaries. 286
 287

Impact of force-velocity tradeoff on feeding and mate choice in small songbirds 288

In this study, we found that domestic canaries move their beak at frequencies of 18 ± 4 Hz, with a maximum of 25 Hz. As hypothesized, 289
 this matches the reported frequencies of peak trill rates in singing canaries (Drăgănoiu et al., 2002). The observed frequencies correspond 290
 to the fastest trill rates observed in Darwin's finches (cf. Podos, 2001). These observations imply that the force-velocity tradeoff in beak 291
 movement described in singing songbirds also affects feeding performance, allowing birds with low bite forces to produce fast syllable 292
 rates and to apply extremely rapid and efficient seed processing. This is plausible in the light of sexual selection. Female domestic 293
 canaries have a clear preference for elaborate birdsong and use syllable rate as a criterion for mate choice (Drăgănoiu et al., 2002). Based 294
 on the 'honest signaling theory', we hypothesize that this might be related to the fact that fast-singing males are also highly efficient in 295
 processing small seeds, proving to be able to meet their high energy demands despite their low bite force and be successful in producing 296
 healthy offspring. This hypothesis is based on previous comparative studies reporting that small-billed birds sing faster (Podos, 2001; 297
 Herrel et al., 2009) and process small seeds more efficiently (Abbott et al., 1975; Smith, 1987) than large-billed birds. 298

Relevance of 3D mandible movement 299

We have shown that domestic canaries use specific three-dimensional mandible movements during the different phases of seed process- 300
 ing. An increased usage of medio-lateral movement during biting and dehusking confirms our hypothesis and is in line with previously 301
 reported observations in other fringillid finches (Ziswiler, 1965; Nuijens and Zweers, 1997; van der Meij and Bout, 2006). Using a wide 302
 range of motion during seed cracking and dehusking allows for a more efficient way of feeding; the husk is removed skillfully without 303
 crushing the seed into pieces, which would involve loosing parts of the seed. 304
 Medio-lateral movement of the mandible is not exclusive to feeding. It is also utilized for preening and nest preparation (Kear, 1962), 305
 which highlights the importance of a highly kinetic skull for the multiple tasks of a bird beak. The occurrence of medio-lateral movement 306
 of the lower beak in birds has been linked to certain morphological characteristics of the cranium, e.g., ligaments and muscle properties 307
 (Nuijens and Zweers, 1997). For example, the absence of a PO ligament in Fringillid finches has been suggested to facilitate medio- 308
 lateral movement of the mandible (Nuijens and Bout, 1998). The present study provides further evidence for that. 309
 310

Conclusion 311

Our analyses of beak movement during seed processing has revealed that there is no obligate coupling of maxilla and mandible movement 312
 in domestic canaries. The birds use specific three-dimensional beak movements during the different phases of seed processing, showing 313
 variation in correlation of upper and lower jaw as well as in relative directions of mandible movement. During seed positioning, the 314
 beak moved at frequencies matching the reported frequencies of peak trill rates in singing canaries, hinting at the joint dependence of 315
 singing and feeding on mechanical properties and constraints of the cranial system. Males and females did not show differences in any 316
 of the derived parameters, suggesting that there is no sexual dimorphism in beak movement during feeding in domestic canaries. Further 317
 research is needed to identify how the underlying cranial system generates beak movement in domestic canaries and what the effects of 318
 the absence or presence of a PO ligament are for beak movement in granivorous songbirds in general. 319

LIST OF SYMBOLS AND ABBREVIATIONS 320

ΔX , ΔY , ΔZ : medio-lateral, antero-posterior, and dorso-ventral displacement of beak markers from their reference position on the 321
 closed beak; C_{pool} , F_{pool} , M_{pool} : statistical models of beak correlation (C), mandible frequency (F), and 3D mandible displacement 322
 (M) fitted to the pooled data; C_{sex} , F_{sex} , M_{sex} : statistical models of beak correlation (C), mandible frequency (F), and 3D mandible 323
 displacement (M) including 'sex' as a categorical variable; C_{ph} , M_{ph} : statistical models of beak correlation (C) and 3D mandible 324
 displacement (M) including 'phase' as a categorical variable; $C_{sex,ph}$, $M_{sex,ph}$: statistical models of beak correlation (C) and 3D 325

326 mandible displacement (M) including both 'sex' and 'phase' as categorical variables; $C_{sex/ph}$, $M_{sex/ph}$: statistical models of beak
327 correlation (C) and 3D mandible displacement (M) including all combinations of 'sex' and 'phase' as categorical variables; c : correlation
328 coefficient; f : frequency of dorso-ventral movement of the mandible; m_x, m_y, m_z : percental displacement of mandible in x-, y-, and
329 z-direction; α : model parameter defining the intercept of the linear models; β : model parameter defining the slopes of the linear models;
330 ϵ : model parameter defining the residuals of the linear models; ν_{male}, ν_{ph} : boolean vectors defining which data rows are from male
331 birds or from the phase 'ph'; PO ligament: postorbital ligament.

332 Acknowledgements

333 We want to thank Prof. Dr. Wendt Müller from the Behavioural Ecology and Ecophysiology Research group at the University of Antwerp for providing the birds for this
334 study. Furthermore, we thank Peter Scheys for animal care and for helpful advice on animal welfare and handling and Jan Scholliers for building the glass recording
335 cages and feeders for the experiments. Finally, we thank three anonymous reviewers for their constructive comments on the manuscript.

336 Competing interests

337 No competing interests declared.

338 Contribution

339 Conceptualization: S.V.W.; Methodology: M.M., S.V.W.; Software: M.M.; Formal analysis: M.M.; Investigation: M.M.; Resources: S.V.W.; Data Curation: M.M.; Writing –
340 original draft preparation: M.M.; Writing – review and editing: M.M., S.V.W.; Visualization: M.M.; Supervision: S.V.W.; Funding acquisition: M.M., S.V.W.

341 Funding

342 This study was funded by Fonds Wetenschappelijk Onderzoek (FWO PhD fellowship 1113521N to M.M. and grant 1505819N to S.V.W.) and by grant from the University
343 of Antwerp (SEP BOF FFB190380 & FFB180316 to S.V.W.).

344 Data availability

345 The Procrustes-aligned beak movement data (ΔX , ΔY , ΔZ) and kinematic parameters (correlation, frequency, and three-dimensional mandible displacement) together
346 with the statistical analysis (Python script) are available in Dryad (https://datadryad.org/stash/share/Iha4U7pIlykdmMMLrmM7ytBXRd0hdZn_OAPDG97r1Y).

347 Supplementary

348 The supplementary material contains an example video of one of the analyzed feeding events (MovieS1.mp4).

349 REFERENCES

- 350 Abbott, I., Abbott, L. K. and Grant, P.R. (1975). Seed selection and handling ability of four species of Darwin's finches. *Condor*. **77**, 332–335.
- 351 Benkman, C. W. and Pulliam, H. R. (1988). The comparative feeding rates of North American sparrows and finches. *Ecology*. **69**, 1195–1199.
- 352 Bock, W. J. (1964). Kinetics of the avian skull. *J. Morphol.* **114**, 1–41.
- 353 Bout, R. and Zeigler, H. P. (1994). Jaw muscle (EMG) activity and amplitude scaling of jaw movements during eating in pigeon (*Columba livia*). *J. Comp. Physiol. A*. **174**, 433–442.
- 354 Bout, R. G. and Zweers, G. A. (2001). The role of cranial kinesis in birds. *Comp. Biochem. Phys. A*. **131**, 197–205.
- 355 Dawson, M. M., Metzger, K. A., Baier, D. B. and Brainerd, E. L. (2011). Kinematics of the quadrate bone during feeding in mallard ducks. *J. Exp. Biol.* **214**, 2036–2046.
- 356 Drăgănoiu, T. I., Nagle, L. and Kreutzer, M. (2002). Directional female preference for an exaggerated male trait in canary (*Serinus canaria*) song. *P. Roy. Soc. Lond. B Bio.* **269**, 2525–2531.
- 357 Fisher, H. I. (1955). Some aspects of the kinetics in the jaws of birds. *Wilson Bull.* 175–188.
- 358 Genbrugge, A., Herrel, A., Boone, M., Van Hoorebeke, L., Podos, J., Dirckx, J., Aerts, P. and Dominique, A. (2011). The head of the finch: the anatomy of
359 the feeding system in two species of finches (*Geospiza fortis* and *Padda oryzivora*). *J. Anat.* **219**, 676–695.
- 360 Genbrugge, A., Adriaens, D., De Kegel, B., Brabant, L., Van Hoorebeke, L., Podos, J., Dirckx, J., Aerts, P. and Herrel, A. (2012). Structural tissue
361 organization in the beak of Java and Darwin's finches. *J. Anat.* **221**, 383–393.
- 362 Grant, P. (1981). The feeding of Darwin's finches on *Tribulus cistoides* (L.) seeds. *Anim. Behav.* **29**, 785–793.
- 363 Grant, P. R. and Grant, B. R. (1995). Predicting microevolutionary responses to directional selection on heritable variation. *Evolution* **49**, 241–251.
- 364 Gussekloo, S.W., Vosselman, M.G. and Bout, R.G. (2001). Three-dimensional kinematics of skeletal elements in avian prokinetic and rynchokinetic skulls
365 determined by Roentgen stereophotogrammetry. *J. Exp. Biol.* **204**, 1735–1744.
- 366 Herrel, A., Podos, J., Huber, S. and Hendry, A. (2005). Bite performance and morphology in a population of Darwin's finches: implications for the evolution of
367 beak shape. *Funct. Ecol.* **19**, 43–48.
- 368 Herrel, A., Podos, J., Vanhooydonck, B. and Hendry, A. P. (2009). Force-velocity trade-off in Darwin's finch jaw function: a biomechanical basis for ecological
369 speciation? *Funct. Ecol.* **23**, 119–125.
- 370
- 371
- 372

- Hoese, W. J. and Westneat, M. W.** (1996). Biomechanics of cranial kinesis in birds: Testing linkage models in the white-throated sparrow (*Zonotrichia albicollis*). *J. Morphol.* **227**, 305–320. 373
374
- Huber, S. K. and Podos, J.** (2006). Beak morphology and song features covary in a population of Darwin's finches (*Geospiza fortis*). *Biol. J. Linn. Soc.* **88**, 489–498. 375
376
- Kear, J.** (1962). Food selection in finches with special reference to interspecific differences. In *P. Zool. Soc. Lond.* **138**, 163–204. 377
- Knörlein, B. J., Baier, D. B., Gatesy, S. M., Laurence-Chasen, J. and Brainerd, E. L.** (2016). Validation of XMALab software for marker-based XROMM. *J. Exp. Biol.* **219**, 3701–3711. 378
379
- Neves, D. P., Mehdizadeh, S. A., Santana, M. R., Amadori, M. S., Banhazi, T. M. and de Alencar Nääs, I.** (2019). Young broiler feeding kinematic analysis as a function of the feed type. *Animals* **9**, 1149. 380
381
- Nuijens, F. W. and Bout, R. G.** (1998). The role of two jaw ligaments in the evolution of passerines. *Zoology* **101**, 24–33. 382
- Nuijens, F. W. and Zweers, G. A.** (1997). Characters discriminating two seed husking mechanisms in finches (Fringillidae: Carduelinae) and estrildids (Passeridae: Estrildinae). *J. Morphol.* **232**, 1–33. 383
384
- Podos, J.** (2001). Correlated evolution of morphology and vocal signal structure in Darwin's finches. *Nature* **409**, 185–188. 385
- Python Software Foundation** (2022). Python Language Reference, version 3.10. Available at <http://www.python.org>. 386
- Rohlf, F. J. and Slice, D.** (1990). Extensions of the Procrustes method for the optimal superimposition of landmarks. *Syst. Biol.* **39**, 40–59. 387
- Salvatier, J., Wiecki, T. V. and Fonnesbeck, C.** (2016). Probabilistic programming in Python using PyMC3. *PeerJ Comput. Sci.* **2**, e55. 388
- Smith, T. B.** (1987). Bill size polymorphism and intraspecific niche utilization in an African finch. *Nature* **329**, 717–719. 389
- Soons, J., Herrel, A., Genbrugge, A., Aerts, P., Podos, J., Adriaens, D., de Witte, Y., Jacobs, P. and Dirckx, J.** (2010). Mechanical stress, fracture risk and beak evolution in Darwin's ground finches (*Geospiza*). *Philos. T. Roy. Soc. B.* **365**, 1093–1098. 390
391
- Soons, J., Genbrugge, A., Podos, J., Adriaens, D., Aerts, P., Dirckx, J. and Herrel, A.** (2015). Is beak morphology in Darwin's finches tuned to loading demands? *PloS one* **10**, e0129479. 392
393
- Van Den Heuvel, W. F.** (1991). Kinetics of the skull in the chicken (*Gallus gallus domesticus*). *Neth. J. Zool.* **42**, 561–582. 394
- van der Meij, M. A. and Bout, R. G.** (2000). Seed selection in the Java sparrow (*Padda oryzivora*): preference and mechanical constraint. *Can. J. Zool.* **78**, 1668–1673. 395
396
- van der Meij, M. A. and Bout, R.G.** (2004). Scaling of jaw muscle size and maximal bite force in finches. *J. Exp. Biol.* **207**, 2745–2753. 397
- van der Meij, M. A. and Bout, R. G.** (2006). Seed husking time and maximal bite force in finches. *J. Exp. Biol.* **209**, 3329–3335. 398
- van der Meij, M. A. and Bout, R. G.** (2008). The relationship between shape of the skull and bite force in finches. *J. Exp. Biol.* **211**, 1668–1680. 399
- Van Gennip, E. and Berkhoudt, H.** (1992). Skull mechanics in the pigeon, *Columba livia*, a three-dimensional kinematic model. *J. Morphol.* **213**, 197–224. 400
- Vehtari, A., Gelman, A. and Gabry, J.** (2017). Practical Bayesian model evaluation using leave-one-out cross-validation and WAIC. *Stat. Comput.* **27**, 1413–1432. 401
402
- Virtanen, P., Gommers, R., Oliphant, T. E., Haberland, M., Reddy, T., Cournapeau, D., Burovski, E., Peterson, P., Weckesser, W., Bright, J., et al.** (2020). SciPy 1.0: fundamental algorithms for scientific computing in Python. *Nat. Methods* **17**, 261–272. 403
404
- Westneat, M. W., Long, J., Hoese, W. and Nowicki, S.** (1993). Kinematics of birdsong: functional correlation of cranial movements and acoustic features in sparrows. *J. Exp. Biol.* **182**, 147–171. 405
406
- Ziswiler, V.** (1965). Zur Kenntnis des Samenöffnens und der Struktur des hörnernen Gaumens bei körnerfressenden Oscines. *J. Ornithol.* **106**, 1–48. 407
- Zusi, R. L.** (1967). The role of the depressor mandibulae muscle in kinesis of the avian skull. *Proc. U.S. Natl. Mus.* **123**, 1–28. 408

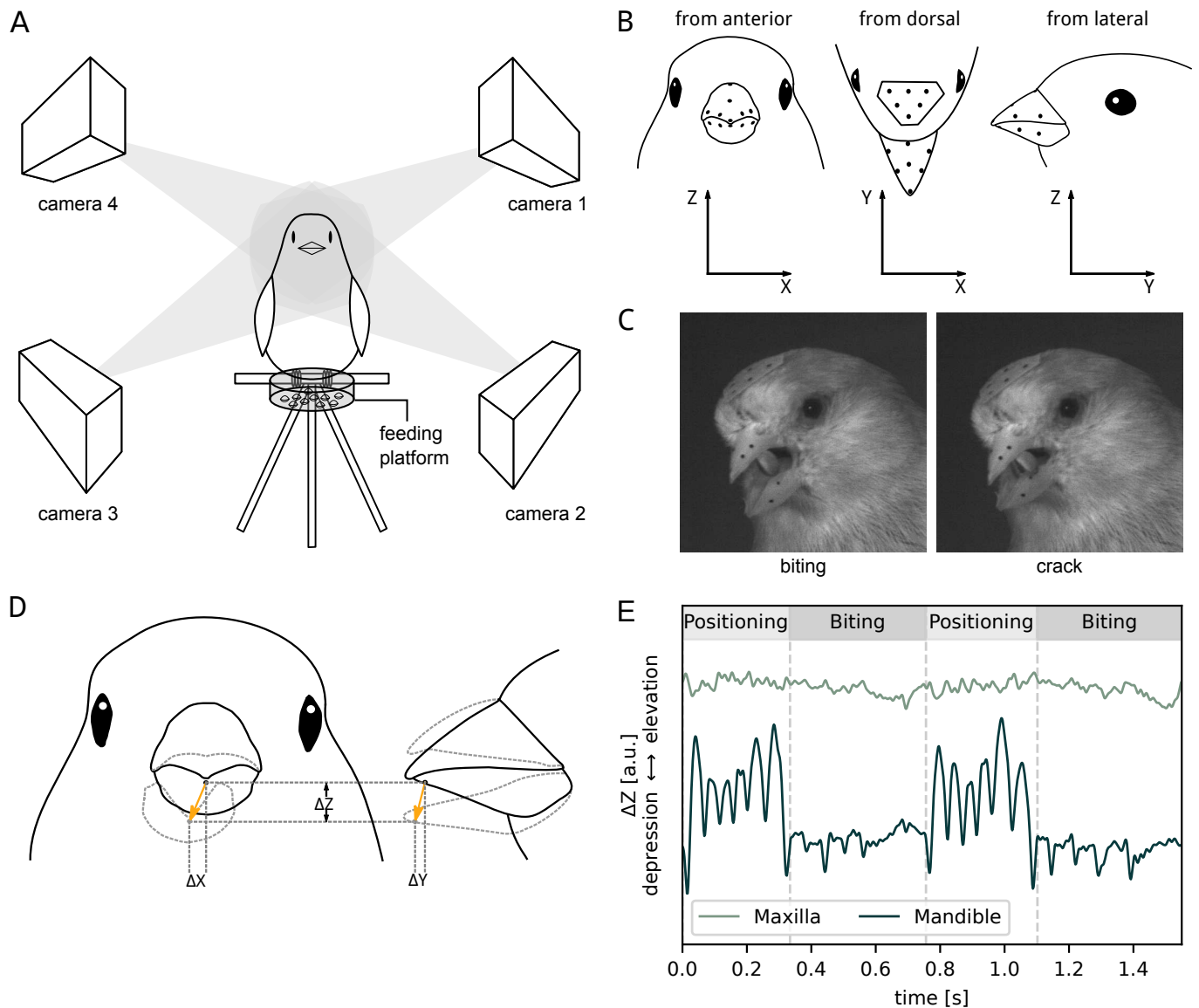


Fig. 1. Experimental setup, marker positions, definition of the reference coordinate system, displacement of the beak relative to the closed beak. (A) Schematic overview of the experimental setup, showing the position of the four cameras relative to the bird. (B) Positions of the markers on maxilla, mandible, and head. The dorsal and ventral markers on maxilla and mandible, respectively, were used to define the YZ-plane of the reference coordinate system. The head markers defined the XY plane. (C) Example frames of a video showing a bird shortly before (left) and after (right) cracking a hemp seed. Images are cropped to the head region. (D) During feeding, each marker moves relative to its reference position on the closed beak in all three dimensions, as exemplified for the ventral marker on the mandible tip. (E) Example trajectory for the dorso-ventral movement ΔZ of maxilla and mandible during alternating positioning and biting phases. Data are low-pass filtered (threshold 60 Hz). See supplementary movie S1 for a full example recording.

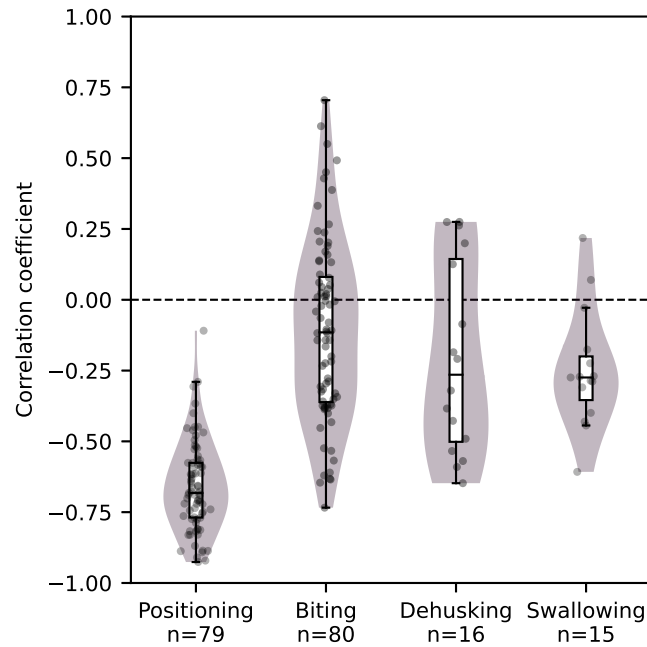


Fig. 2. Coefficient of correlation of dorso-ventral movement of maxilla and mandible during the different phases of seed processing. Negative values indicate opposite movement, positive values parallel movements. The higher the absolute values, the higher the synchronization. Dots indicate raw data, box plots their medians and quartiles, violin plots their kernel densities. Raw data extracted from 16 feeding events of 6 individuals (3 males, 3 females). Beak movement is mostly negatively correlated during positioning and swallowing. The more varying correlation coefficients during dehusking and biting indicate that coupling of beak movement is not obligate in domestic canaries.

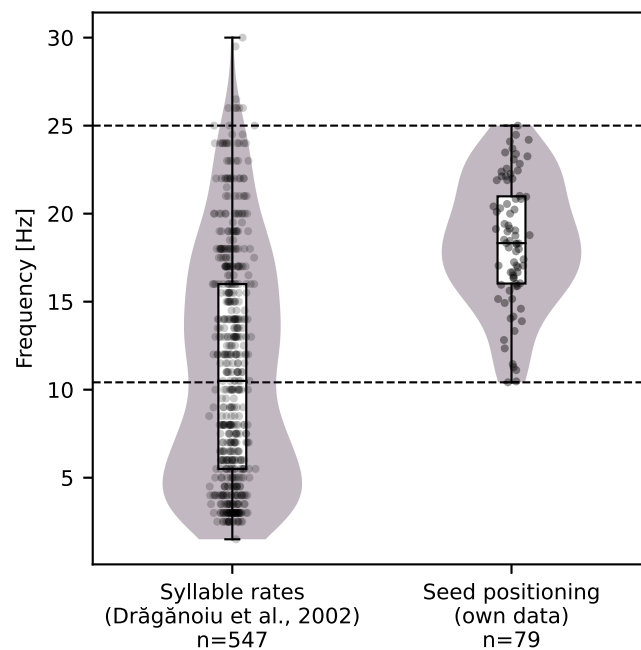


Fig. 3. Beak frequencies of domestic canaries during singing and seed positioning. Syllable rate data from Drăgănoiu et al. (2002). Dots indicate raw data, box plots their medians and quartiles, violin plots their kernel densities. Own data (right) extracted from 16 feeding events of 6 individuals (3 males, 3 females). Our observed data of mandible frequency during seed positioning lie within the range of reported syllable rates, covering values between the 50th and 98th percentile (dashed lines).

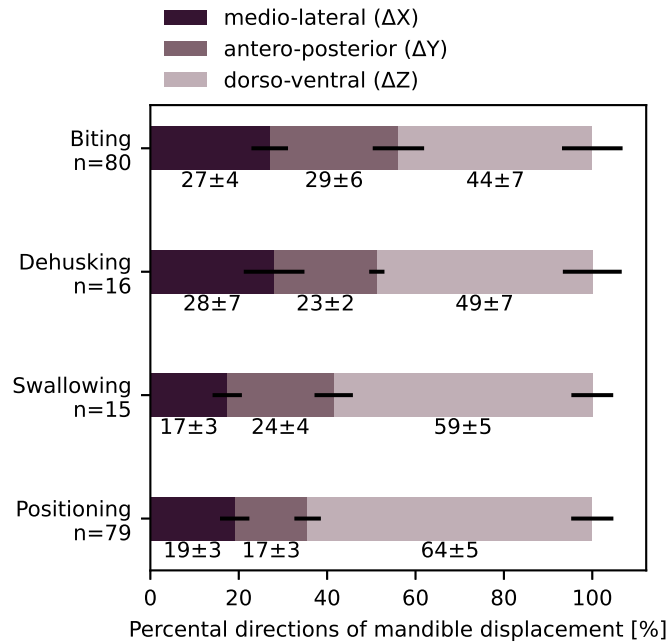


Fig. 4. Percentage (mean ± s.d.) of mandible movement in the three dimensions during the different phases of seed processing. See Eqn 1 and 2 for a description of how data were calculated from the 3D coordinates. Data extracted from 16 feeding events of 6 individuals (3 males, 3 females). Dorso-ventral movement direction is less dominant during biting and dehusking, because more movement occurs medio-laterally compared to swallowing and positioning phases.